PIMMS échelle: the next generation of compact diffraction limited spectrographs for arbitrary input beams

Christopher H. Betters[*a,b], Sergio G. Leon-Saval[a], Joss Bland-Hawthorn[a,b], Samuel N. Richards[b], Tim A. Birks[c] and Itandehui Gris-Sánchez[c]

[a]Institute of Photonics and Optical Science, School of Physics, University of Sydney, Australia
[b]Sydney Institute for Astronomy, School of Physics, University of Sydney, Australia
[c]Department of Physics, University of Bath, Claverton Down, Bath, BA2 7AY, UK

ABSTRACT

PIMMS échelle is an extension of previous PIMMS (photonic integrated multimode spectrograph) designs, enhanced by using an échelle diffraction grating as the primary dispersing element for increased spectral bandwidth. The spectrograph operates at visible wavelengths (550 to 780nm), and is capable of capturing ~100 nm of $\mathcal{R} > 60,000$ ($\lambda/\Delta\lambda$) spectra in a single exposure. PIMMS échelle uses a photonic lantern to convert an arbitrary (e.g. incoherent) input beam into N diffraction-limited outputs (i.e. N single-mode fibres). This allows a truly diffraction limited spectral resolution, while also decoupling the spectrograph design from the input source.

Here both the photonic lantern and the spectrograph slit are formed using a single length of multi-core fibre. A 1x19 (1 multi-mode fiber to 19 single-mode fibres) photonic lantern is formed by tapering one end of the multi-core fibre, while the other end is used to form a TIGER mode slit (i.e. for a hexagonal grid with sufficient spacing and the correct orientations, the cores of the multi-core fibre can be dispersed such that they do not overlap without additional reformatting). The result is an exceptionally compact, shoebox sized, spectrograph that is constructed primarily from commercial off the shelf components. Here we present a brief overview of the échelle spectrograph design, followed by results from on-sky testing of the breadboard mounted version of the spectrograph at the 'UK Schmidt Telescope'.

Keywords: astrophotonics, diffraction limited spectrograph, photonic lantern, high resolution spectrograph,single mode spectrograph

1. INTRODUCTION

Spectroscopy is one of the fundamental techniques in any astronomers tool-kit. With it one can determine a plethora of physical properties including chemical composition, age, distance, temperature and the dynamics of astronomical sources. Conventional astronomical spectrographs often use multi-mode optical fibres (MMFs) to feed light from a telescope to the spectrograph slit. While this has been an extremely successful technique, these spectrographs are inherently limited in their performance (spectral resolution and throughput) by the size of the entrance slit (i.e. a MMF). The PIMMS (photonic integrated multimode spectrograph)[1] concept aims to side step that limitation through the use of the photonic lantern (PL) multi-mode to single-mode converter.[2–6] By augmenting a conventional bulk-optic spectrograph with a PL we can achieve a truly diffraction limited spectral resolution, whilst simultaneously decoupling the optical design from the original input source.

PIMMS échelle is the logical continuation in our work developing a such compact diffraction limited spectrograph. Our first setup, *PIMMS IR*,[7–9] is a relatively simple single order spectrograph, operating in the short wave infrared (1550 nm) based upon the PIMMS#0 concept presented by Bland-Hawthorn *et al.*[1] PIMMS IR's high resolving power (R~30,000) and limited detector size (640×512 pixel array) restricted the bandwidth of a single exposure to ~8 nm. The next generation, PIMMS échelle, has several advantages and improvements over its sibling:

- it operates in visible wavelengths, allowing use of more cost effective large format CCDs, with drastically better noise characteristics compared to the InGaAs array used in PIMMS IR.

[*]c.betters@physics.usyd.edu.au

Ground-based and Airborne Instrumentation for Astronomy V, edited by Suzanne K. Ramsay, Ian S. McLean, Hideki Takami, Proc. of SPIE Vol. 9147, 91471I · © 2014 SPIE · CCC code: 0277-786X/14/$18 · doi: 10.1117/12.2055638

- has a potential resolving power in-excess of 60,000.
- uses a larger lantern, based on a 19 multi-core fibre (MCF).[6,10]
- the primary disperser is an échelle grating. Combined with a volume-phase holographic (VPH) grating cross-disperser we maintain high resolution and throughput, but with significantly increased bandwidth.

The optical layout and a picture of the actual setup are shown in Fig. 1. The whole setup fits (nearly) on a 300 × 600 mm breadboard (a future version folds the setup allowing it to fit within the breadboard area completely). The mounts for both the échelle and cross-disperser are a combination of 3D printed parts and 'off-the-shelf' components (to achieve the correct angles and center the gratings about their rotation axis).

Here we will describe the design of PIMMS échelle, including simulated and measured performance. We then present spectra taken at the UK Schmidt telescope as a visiting instrument, likely the highest resolution spectra ever taken at the telescope.

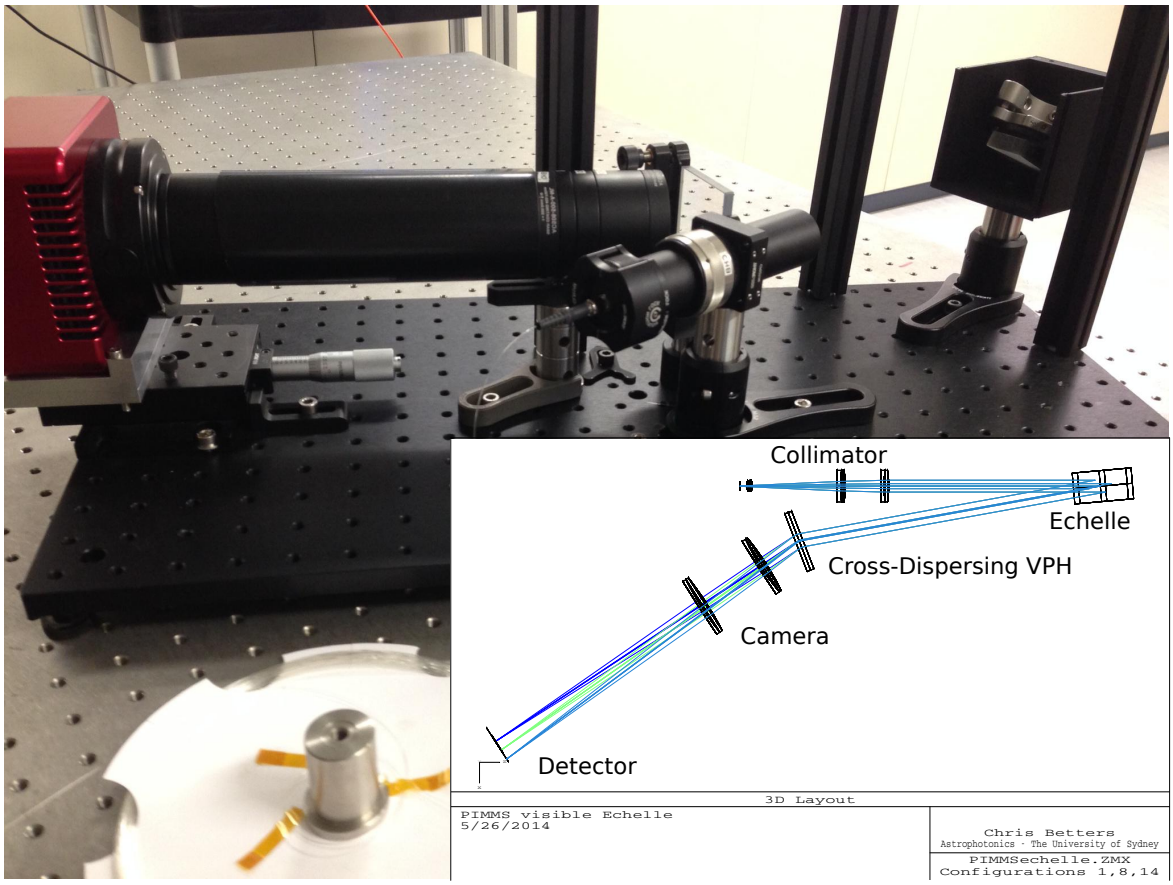

Figure 1: Image of the PIMMS échelle. Inset is the the layout of the optical design. The échelle dispersion is perpendicular to the plane of the page. The échelle is rotated by 5 degrees about the y axis (perpendicular to page) in a quasi-Littrow configuration. The central wavelength of each diffraction order from 73, 79 and 86 is shown.

2. OPTICAL DESIGN

2.1 Pseudo-Slit and Photonic Lantern

We use a 19 MCF to form both the lantern and pseudo-slit of the spectrograph from a single length of fibre. One side is tapered with low index capillary jacket to form the lantern and then connectorised. The other is

connectorised and used directly as the slit. As the cores of our MCF form a hexagonal grid we can form the pseudo-slit directly using the TIGER technique.[9] This technique consists of rotating the core configuration in order to fit as many cores as possible within the detector area. With a core spacing of ~60μm, this allows each core to have an effective separation in the cross-dispersion direction of ~12μm. By keeping the hexagonal geometry we are able to increase the number of fibres in the entrance slit while keeping the overall off-axis distance of all the fibres to a minimum (and thereby eliminate the need for any additional remapping of the SM cores).

An important note, that will effect the final performance of the current setup, is that the MCF and lantern described above and currently used in PIMMS échelle was originally intended for use at 1550 nm. As a result we are currently operating in a 'few-mode' configuration, which essentially results in a broadened PSF. This is not a fundamental issue, just a by product of the TIGER configuration and the particular pre-form used to manufacture the MCF. We did fabricated a visible version of the 19 MCF, however the parameters of this fibre, and in particular the core separation, were not ideal for the spectrograph configuration. The cores of the visible version were simply to close together to disperse without overlapping.

2.2 Diffraction grating

The primary disperser is a 25mm by 50mm échelle grating sourced from the Thorlabs[†] catalogue. It has a line density of 31.6 l/mm with a blaze of 63° (i.e. a dispersion of 14.4 nm/mrad; or an R2 grating). The échelle grating is used in a quasi-Littrow configuration with a $\gamma = 5°$, so the dispersed beam is diverted 10 degrees off-axis from the collimator (a newer version of the setup reduces γ to 2° using a mirror to fold the setup). The 63° angle of incidence and grating size set the first limit on the collimated beam size, it must be < 25 mm or it will overfill. Gaussian beam truncation considerations indicate the $1/e^2$ beam width should be roughly half the aperture.[8,11,12] Thus the $1/e^2$ beam width incident on the échelle should be less the < 12.5 mm.

Similar considerations are normally required for the cross-disperser. However, the most suitable grating (based on dispersion requirements) was a VPH with an equivalent ruling of 600 l/mm blazed for 600 nm from Wasatch Photonics[‡]. This grating is 2" square and is thus not a truncation concern.

For reference, the grating equation in a quasi-Littrow configuration is:

$$m\lambda = d\cos\gamma\,(\sin\alpha + \sin\beta) \tag{1}$$
$$= 2d\cos\gamma\sin\alpha \tag{2}$$

where α and β are incidence and diffraction angles and γ is rotation of the grating. The γ angle can be thought to effectively reduce the line density by small amount.

2.3 Collimator

The collimator takes some inspiration from amici lens design proposed Robertson and Bland-Hawthorn.[12] I instead use a small short focal length achromat to slow the beam, and compelete the collimation with two larger achromats. The final design is composed of a ϕ 8mm doublet with an EFL of 20mm combined with two ϕ 1" doublets with EFLs of 200mm. Combined they have an EFL of 64.7mm (f/2.5 overall). Here it is operating at ~f/6 to give a collimated beam of 10mm ($1/e^2$ diameter).

2.4 Camera

The camera is a simple pair of 2" achromatic doublets with EFLs of 400 and 500 mm respectively. Combined there EFL is 237 mm (f/4.6 overall). Here it is operating at closer to f/20. The overall optical layout of the design is shown in Fig. 1. This results in a magnification of ~3.6. Overall the optics are diffraction limited from 500nm thought to 800nm (in 100nm blocks). Blue-ward and red-ward of the those limits has not been explored as yet.

[†] http://www.thorlabs.com

[‡] http://www.wasatchphotonics.com

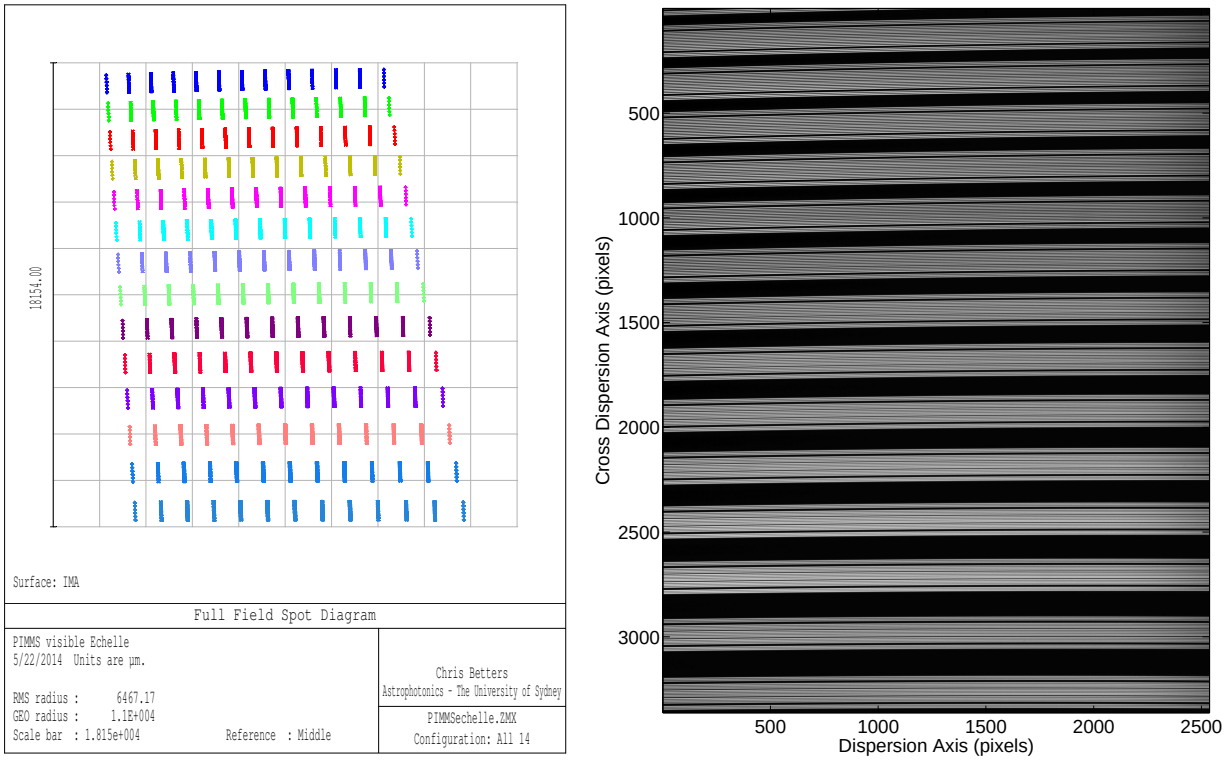

(a) (b)

Figure 2: In both: x axis is échelle dispersion, y-axis is cross dispersion. *a)* Full-field ray-trace of a 0.3mm long slit for orders 73-86. Wavelength span the FSR of each order. *b)* Halogen lamp flat field frame. Contrast was enhanced to clearly see the reddest orders.

2.5 Detector

The detector package is an Atik 383L+[§], nominally marketed for small telescope astrophotography. The sensor is the 8-megapixel Kodak KAF-8300 CCD (3362×2504, with a pitch of 5.4μm) . It has a low read noise ($\sim< 10e^-$) and dark current ($\sim$0.05 e^-/s @ $-10°$C). The large format coupled with the small pixels make it ideal for the échelle design. An additional benefit is the low cost ($\sim$\$2000) and wide availability.

2.6 Detector Utilisation and Wavelength coverage

With the above sensor, PIMMS échelle can capture up to 16 orders in a single frame, depending on the configuration of the cross-disperser and camera/detector. The order separation after being cross-dispersed allows enough room for a $\sim$300 micron slit, or the 1×19 TIGER MCF, up to a blue limit of around 550nm. While in the red end of the spectrum we are limited to around 780nm, primarily by the VPH efficiency. The setup used on sky at the UKST contained 14 orders (73 to 86), covering 655nm to 770nm. A ZEMAX ray trace of this configuration is shown in Fig. 2a. Each order is represented by 4 field positions, along the extent of the slit and 9 wavelengths cover the free spectral range (FSR; $\lambda_{\text{central}}/m$) The detector is rotated 4.5° to align the each order with detector columns, and to allow more complete filling of the sensor. Fig. 2b is a flat field image taken using a halogen lamp. Each order contains 19 spectra corresponding to the cores of the MCF.

[§] `http://www.atik-cameras.com`

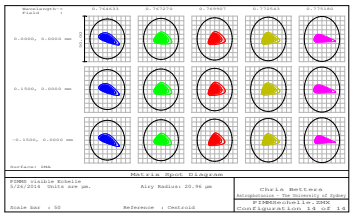

(a) Spot Diagram - Order 73

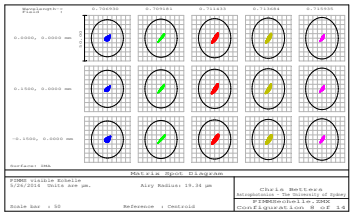

(b) Spot Diagram - Order 79

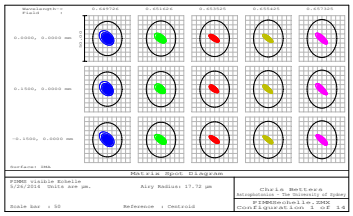

(c) Spot Diagram - Order 86

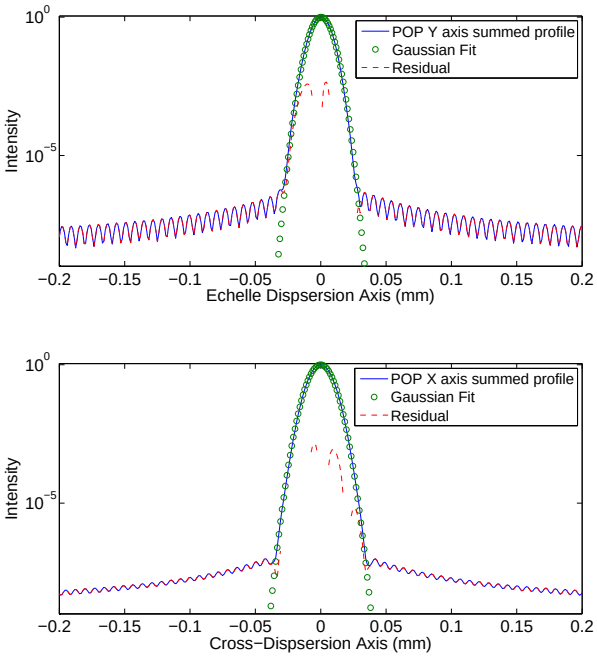

(d) Typical Physical Optics Simulation

Figure 3: *a-c)* Spot Diagrams across pseudo-slit for orders 73, 79 and 86 (top, center and bottom of detector). Wavelengths in each diagram cover the FSR ($\lambda_{\text{central}}/m$) of each order. The black oval is the indicative airy-disk. All bounding boxes are 50μm square. *d)* The solid (blue) lines are profile in the dispersion (top) and cross-dispersion (bottom) axes of a typical Physical Optics Simulation (POP). The circle markers (green) show the best fit gaussian, the dashed line (red) line shows the fit residual. In both axes the the profiles are well matched by the Gaussian down to $\sim 10^{-5}$ levels, indicating there are no significant broadening effects from the simulated optical system.

2.7 Image Quality

2.7.1 Simulation

All the optics have been selected to produces a diffraction limited image of the slit across the detector. Fig. 3a-c are ZEMAX spot diagrams for orders 73, 80 and 86 (covering each edge and the center of the CCD). The spread of wavelengths cover the FSR of each order. Across the detector ray tracing indicates diffraction limited performance, and indeed, as can be seen in Fig. 3d, physical optics simulations support this. We can thus use physical optics to get a realistic estimation of the maximum possible resolution achievable with PIMMS échelle.

In Fig. 4a we show the results of such simulations. Here ZEMAX was scripted to produces a physical optics propagation (POP) simulations for several wavelengths across the FSR of each diffraction order and to save corresponding dispersion from ray tracing and chief ray position position in the image. The POP simulations widths are then determined using a 2D Gaussian fit. The bottom of Fig. 4a shows the FWHM across the detector, it relatively constant, but increases slightly as it shifts toward the red. The top shows the corresponding resolving power, defined as $\lambda/(\text{FWHM} \times \text{dispersion} \times 1.119)$. The dispersion is estimated using ray tracing, while the factor 1.119 provides a more realistic measure of the true resolving power (FWHM$\times$1.119 is the offset required between two Gaussians to have the same contrast that would be obtained using the Rayleigh criterion[13]).

2.7.2 Measured

To wavelength calibrate PIMMS échelle we use a thorium argon hollow cathode lamp. This provides numerous lines in each diffraction order allowing a well defined wavelength scale. In Fig. 4b the lines of the Thorium Argon lamp are used to measure the PSF across the detector. Similar to Fig. 4a, the bottom shows the fitted FWHM of each the brighter lines in the spectrum. The first thing to note is the larger average FWHM, round 4-5 pixels. This is roughly as was expected from the use of the nominally infrared MCF lantern. Further, the simulations do not include issues such as grating quality or variations between the prescriptions and the real system (although the effect of the later should be minimal). During setup of the optical system (and as a sanity check) the camera and collimator imaged (that is a system without the dispersing elements) the visible version of our MCF and returned PSFs consistent with the simulations. Nonetheless, even in this 'few-mode' configuration, PIMMS échelle has achieves a resolving power $> \sim 30,000$ over essentially the entire echellogram.

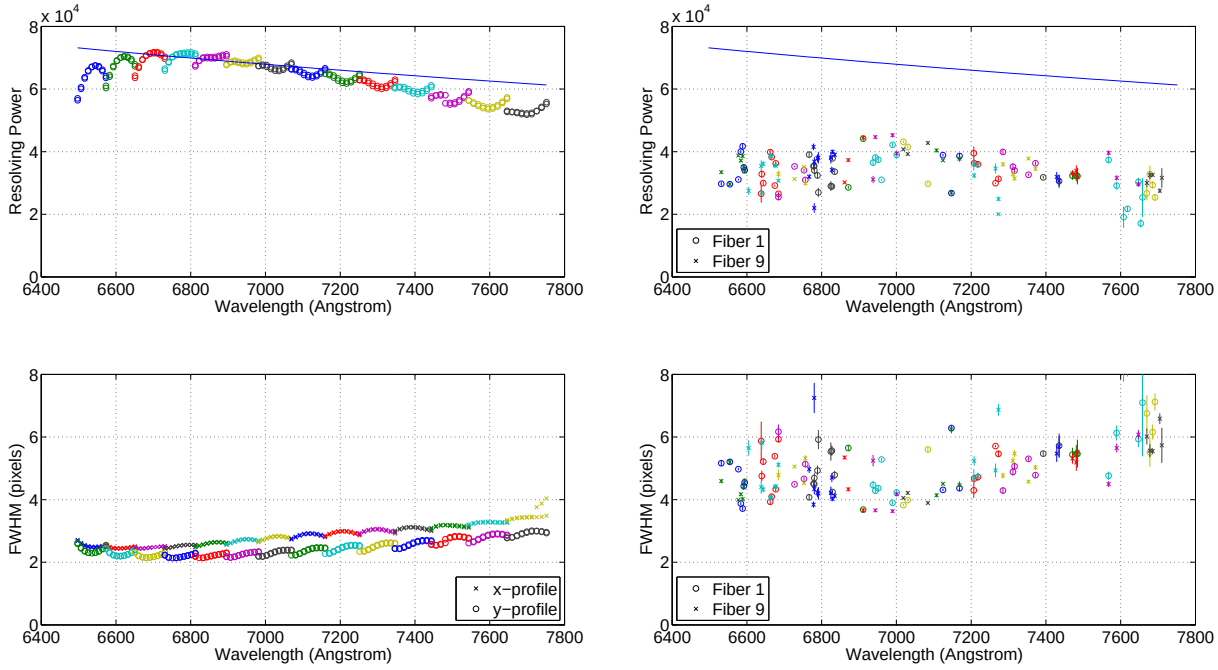

(a) Estimated PSF FWHM and Resolving Power

(b) Meaured PSF FWHM and Resolving Power

Figure 4: *a)* POP simulations are completed for 9 wavelengths covering the FSR of each order and for field positions at the center and edge of a 300μm pseudo-slit. These plots show the fitted FWHM (bottom) of each Gaussian and the corresponding resolving power (top). Changes in colour (and arc) indicate each diffraction order. The resolving power is defined as $\lambda_0/(1.119 \times \text{FWHM})$.

3. ON-SKY AT UKST

In late April 2014 we took PIMMS échelle to the UK Schmidt telescope (UKST) as part preliminary testing for TAIPAN and starbugs.[14] We had a rather straight forward goal: obtain stellar spectra with a measurable radial velocity. To that end we had two methods of coupling light from the telescope focus to the lantern. The first used a coherent fibre bundle[15] while the second simply placed the lantern's MM input directly at the focus.

The coherent fibre bundles reproduces an input image at its output. Thus a guide star can be re-imaged from the focal plane of the telescope to a guider camera without additional optics in the telescope. We took the additional step of cutting a simple v-groove into a bundle to hold a 50/125 MMF. This MMF was then coupled to the MM input of the PIMMS échelle lantern. This technique was particularly useful as it provided visual feed back of the location of the target star in the focal plane, allowing us to quickly position it on the 'science fibre'.

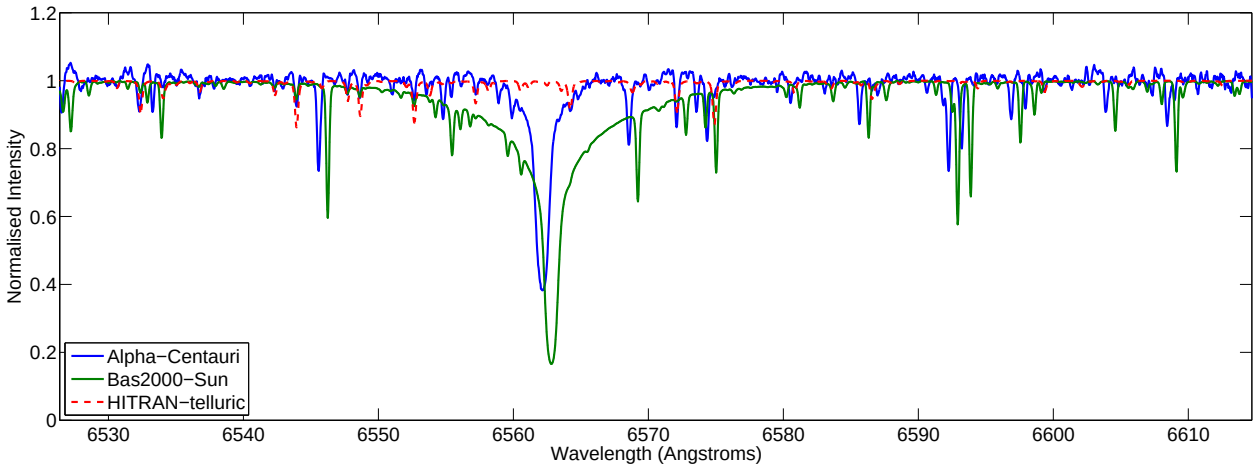

(a) Order 86

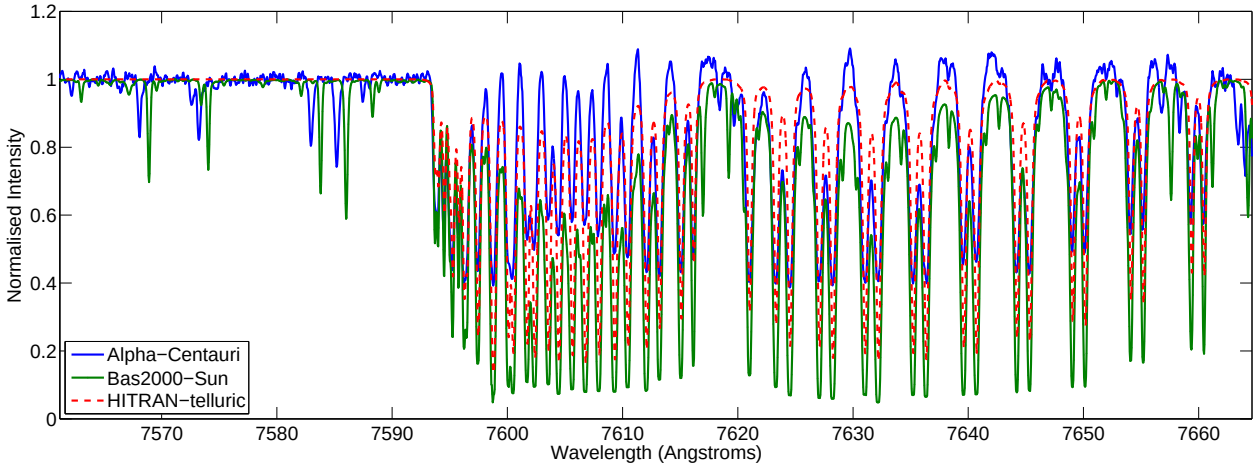

(b) Order 74

Figure 5: Shown in each panel: α-Cen (blue), HITRAN telluric (red) and bas2000 (solar) *a)* Order 86 — Main feature is H-alpha. Note the continuum fit seems to have been overly aggressive, hence the more narrow line in α-Cen spectrum. *b)* Primary feature is the atmospheric O_2 A-band. These lines are of course not shifted and thus provide a sanity check for the wavelength solution.

During target acquisition the collimated beam of the spectrograph is diverted to a smaller camera/CCD for use as intensity monitor, allowing us to maximise the coupling to the lantern.

Given that our previous papers have generally used the solar spectrum as a demonstration spectrum, we decided to work our way out from there, obtaining spectra of Alpha-Centauri (α-Cen). Shown in Fig. 5 are spectra for orders 85, 86 and 74 from a single core of the MCF slit. In each panel you can see the spectrum of α-Cen (blue), HITRAN telluric lines (red)[16] and a solar spectrum from `bass2000.obspm.fr` (green),[17] all normalised such that the continuum is at one. In all three regions we can see that some of the absorption lines in the α-Cen spectra are blue shifted with respect to the solar spectrum. By cross-correlating the solar spectrum with the spectra of α-Cen we get an average shift of 30.9 ± 0.8 km/s (0.07 ± 0.003 nm). Cross-correlating with the telluric spectrum gives an average shift of 0.006 ± 0.8 km/s. The 0.8 km/s uncertainty seems to be tied to variations in the wavelength solution between orders and fibres.

4. CONCLUSIONS

We have briefly presented the PIMMS échelle diffraction limited spectrograph. Its design is diffraction limited over 550 to 780 nm in ~100-120 nm slices. The main limitation in the current setup is the use of the infrared photonic lantern. Even so, its achieves a resolving power on the order of 30,000 across an entire spectrum, in an extremely compact and low cost package. Our next step, beyond a true visible wavelength lantern, is to explore the limits of the designs stability in detail and provide a temperature and pressure controlled environment.

Author contributions

CHB, SLS and JBH have developed and overseen the PIMMS project. CHB wrote the manuscript and designed/built PIMMS échelle. CHB and SNR performed the on-sky experiments at the UKST. SLS, IGS and TAB designed and fabricated the 19 MCF. CHB and SLS fabricated the 19 MCF photonic lantern.

ACKNOWLEDGMENTS

Authors would like to thank Jon Lawrence at AAO for use of equipment and the opportunity to observe at the UKST.

REFERENCES

[1] Bland-Hawthorn, J. et al., "PIMMS: photonic integrated multimode microspectrograph," *Proc. SPIE* **7735**, 77350N (July 2010).

[2] Leon-Saval, S. G., Argyros, A., and Bland-Hawthorn, J., "Photonic lanterns," *Nanophotonics* **2**(5-6), 429–440 (2013).

[3] Leon-Saval, S. G., Argyros, A., and Bland-Hawthorn, J., "Photonic lanterns: a study of light propagation in multimode to single-mode converters," *Optics Express* **18**, 8430 (2010).

[4] Leon-Saval, S. G., Birks, T. A., Bland-Hawthorn, J., and Englund, M., "Multimode fiber devices with single-mode performance," *Optics Letters* **30**(19), 2545–2547 (2005).

[5] Noordegraaf, D., Skovgaard, P. M., Nielsen, M. D., and Bland-Hawthorn, J., "Efficient multi-mode to single-mode coupling in a photonic lantern," *Optics Express* **17**(3), 1988–1994 (2009).

[6] Birks, T. A., Mangan, B. J., Díez, A., Cruz, J. L., and Murphy, D. F., ""Photonic lantern" spectral filters in multi-core Fiber," *Optics Express* **20**(13), 13996 (2012).

[7] Betters, C. H., Leon-Saval, S. G., Robertson, J. G., and Bland-Hawthorn, J., "Beating the classical limit: A diffraction-limited spectrograph for an arbitrary input beam," *Optics Express* **21**(22), 26103 (2013).

[8] Betters, C. H., Leon-Saval, S. G., Bland-Hawthorn, J., and Robertson, G., "Demonstration and design of a compact diffraction limited spectrograph," *Proc. SPIE* **8446**, 84463H (September 2012).

[9] Leon-Saval, S. G., Betters, C. H., and Bland-Hawthorn, J., "The Photonic TIGER: a multicore fiber-fed spectrograph," *Proc. SPIE* **8450**, 84501K (September 2012).

[10] Birks, T., Mangan, B., Diez, A., Cruz, J.-L., Leon-Saval, S., Bland-Hawthorn, J., and Murphy, D., "Multicore optical fibres for astrophotonics," *CLEO/Europe and EQEC 2011 Conference Digest* , JSIII2_1, Optical Society of America (2011).

[11] Belland, P. and Creen, J. P., "Changes in the characteristics of a Gaussian beam weakly diffracted by a circular aperture," *Applied Optics* **21**(3), 522–527 (1982).
[12] Robertson, J. G. and Bland-Hawthorn, J., "Compact high-resolution spectrographs for large and extremely large telescopes: using the diffraction limit," *Proc. SPIE* **8446**, 844623 (September 2012).
[13] Robertson, J. G., "Quantifying Resolving Power in Astronomical Spectra," *PASA* **30**, 48 (2013).
[14] Kuehn, K. et al., "Taipan: optical spectroscopy with starbugs," *Proc. SPIE* **9147**, 9147–35 (2014).
[15] Zheng, J. R., Richards, S. N., Goodwin, M., Lawrence, J., Leon-Saval, S. G., and Argyros, A., "A miniature curvature sensor with coherent fiber image bundle," *Proc. SPIE* **9148**, 9148–83 (2014).
[16] Rothman, L. S. et al., "The HITRAN 2008 molecular spectroscopic database," *J. Quant. Spec. Radiat. Transf.* **110**(9-10), 533–572 (2009).
[17] Delbouille, L., Neven, L., and Roland, G., "Photometric atlas of the solar spectrum from l 3000 to l 10000," (1973-1988).